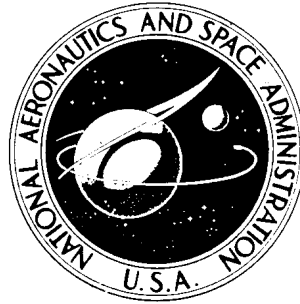# NASA TECHNICAL NOTE

NASA TN D-5827

NASA TN D-5827

# INVESTIGATION OF A DIGITAL
# SIMULATION OF THE XB-70 INLET AND
# ITS APPLICATION TO FLIGHT-EXPERIENCED
# FREE-STREAM DISTURBANCES AT
# MACH NUMBERS OF 2.4 TO 2.6

*by Robert J. Gallagher*

*Flight Research Center*
*Edwards, Calif. 93523*

| 1. Report No. NASA TN D-5827 | 2. Government Accession No. | 3. Recipient's Catalog No. |
|---|---|---|
| 4. Title and Subtitle INVESTIGATION OF A DIGITAL SIMULATION OF THE XB-70 INLET AND ITS APPLICATION TO FLIGHT-EXPERIENCED FREE-STREAM DISTURBANCES AT MACH NUMBERS OF 2.4 TO 2.6 | | 5. Report Date June 1970 |
| | | 6. Performing Organization Code |
| 7. Author(s) Robert J. Gallagher | | 8. Performing Organization Report No. H-585 |
| 9. Performing Organization Name and Address NASA Flight Research Center P. O. Box 273 Edwards, California 93523 | | 10. Work Unit No. 126-15-02-03-24 |
| | | 11. Contract or Grant No. |
| 12. Sponsoring Agency Name and Address National Aeronautics and Space Administration Washington, D. C. 20546 | | 13. Type of Report and Period Covered Technical Note |
| | | 14. Sponsoring Agency Code |

15. Supplementary Notes

16. Abstract

The capability of a digital inlet simulation program to predict both the performance of the started XB-70 inlet system at free-stream Mach numbers of 2.4 to 2.6 and the dynamic aspects of an inlet unstart at these Mach numbers was analyzed. The simulation-predicted performance was compared with flight measurements, and reasonable agreement was obtained for started and unstarting inlet modes. The agreement between empty-fill (buzz) simulations and flight data was less precise. This was attributed to the need for additional information on the boundary-layer-separation process during this mode of inlet operation.

The simulation program was used to determine the reaction of the started inlet over a range of performance levels to free-stream temperature gradients in smooth air and in clear-air turbulence. Atmospheric-temperature variations were found to be nearly as significant as severe turbulence for operation of that type of inlet. Unstart margins for the manually controlled XB-70 inlet in the presence of these disturbances were obtained through use of the simulation program.

| 17. Key Words Suggested by Author(s) Atmospheric turbulence - Propulsion, Inlets - System dynamic simulation | | 18. Distribution Statement Unclassified - Unlimited | | |
|---|---|---|---|---|
| 19. Security Classif. (of this report) Unclassified | 20. Security Classif. (of this page) Unclassified | | 21. No. of Pages 26 | 22. Price * $3.00 |

*For sale by the Clearinghouse for Federal Scientific and Technical Information, Springfield, Virginia 22151

# INVESTIGATION OF A DIGITAL SIMULATION OF THE XB-70 INLET AND ITS APPLICATION TO FLIGHT-EXPERIENCED FREE-STREAM DISTURBANCES AT MACH NUMBERS OF 2.4 TO 2.6

Robert J. Gallagher
Flight Research Center

## INTRODUCTION

As aircraft speeds advance into the supersonic region above a Mach number of 2, dynamic problems in the air-induction system become prominent, and dynamic simulations of such systems are needed to avoid costly design errors. One such simulation, developed by the General Electric Company and North American Aviation, Inc. (refs. 1 to 3), was used extensively during the design and development of the propulsion system for the XB-70 aircraft. The simulation, incorporating the General Electric Dynasar (ref. 1) program, was based on one-dimensional gas dynamic theory and wind-tunnel data. The program was designed for use on a high-speed digital computer. In addition to inlet and duct characteristics, there were provisions for simulating the jet-engine characteristics, although they were not used in this study.

During flights of the XB-70 aircraft, clear-air turbulence and atmospheric temperature gradients were encountered that required unexpected inlet adjustments to avoid inlet unstarts. Because dynamic data were available on the inlet conditions during the time of these disturbances, it was decided to conduct a comparable simulation program to verify the simulation and to determine its applicability to the determination of the dynamic behavior of an air-induction system under adverse free-stream conditions.

The simulation program was conducted by the NASA Flight Research Center using the digital computer facilities of the NASA Ames Research Center. This report presents results from the program and compares them with flight data taken at altitudes of 60,000 feet (18,300 meters) to 65,000 feet (19,800 meters) and at a nominal free-stream Mach number of 2.5. These data were obtained during early Air Force tests to determine aircraft performance (ref. 4) and in later NASA research flights. Simulation results are included that show the reaction of the manually controlled inlet to the turbulence and temperature disturbances over a range of inlet performance levels and, also, the unstart margins required for stable operation. The results encompass information on the control inputs which would be required if a high-performance, automatically controlled inlet were used.

## SYMBOLS

A          duct cross-sectional area normal to flow direction, $ft^2$ $(m^2)$

$a_n$         normal acceleration at airplane center of gravity, g

c         speed of sound, ft/sec (m/sec)

g         acceleration due to gravity, $ft/sec^2$ $(m/sec^2)$

h         altitude, ft (m)

M         Mach number, V/c

m         mass, lb (kg)

$\dot{m}$         mass flow rate, lb/sec (kg/sec)

$m_x'$         relative upstream Mach number

$m_y'$         relative downstream Mach number

p         pressure, $lb/in.^2$ $(N/m^2)$

SPR         shock position ratio, $p_s/p_{impact}$ (fig. 4)

T         temperature, °R (°K)

t         time, sec

V         velocity, ft/sec (m/sec)

W         inlet geometric throat width, in. (cm)

$\bar{\underline{x}}$         shock position, in. (cm)

$\alpha$         angle of attack, deg

$\beta$         angle of sideslip, deg

$\Delta$         incremental change

$\eta$         engine-face total-pressure recovery, $p_{t_2}/p_{t_\infty}$

$\Delta\eta$         change in engine-face total-pressure recovery relative to a specified reference level

Subscripts:

d         conditions in duct volume (fig. 4)

i         initial conditions

2

| s | static conditions |
|---|---|
| t | total conditions |
| x | conditions just upstream of a shock wave |
| y | conditions just downstream of a shock wave |
| ∞ | free-stream conditions |
| * | critical conditions (i.e., conditions where local speed is equal to local speed of sound) |
| 2 | station 2 engine-face plane |

## XB-70 AIRPLANE

Two XB-70 airplanes were built and were designated the XB-70-1 and XB-70-2. The airplane (fig. 1) was originally designed as a long-range, supersonic-cruise, strategic bomber with a design gross weight in excess of 500,000 pounds (2,200,000 newtons), design cruising speed of Mach 3 at 70,000 feet (21,300 meters) to 80,000 feet (24,400 meters) and intercontinental range. It featured a thin, low-aspect-ratio, 65.6°-swept-back leading-edge delta wing with folding wing tips, twin vertical stabilizers with rudders, elevon surfaces for pitch and roll control, and a movable canard with trailing-edge flaps. The airplane is described in detail in references 5 and 6.
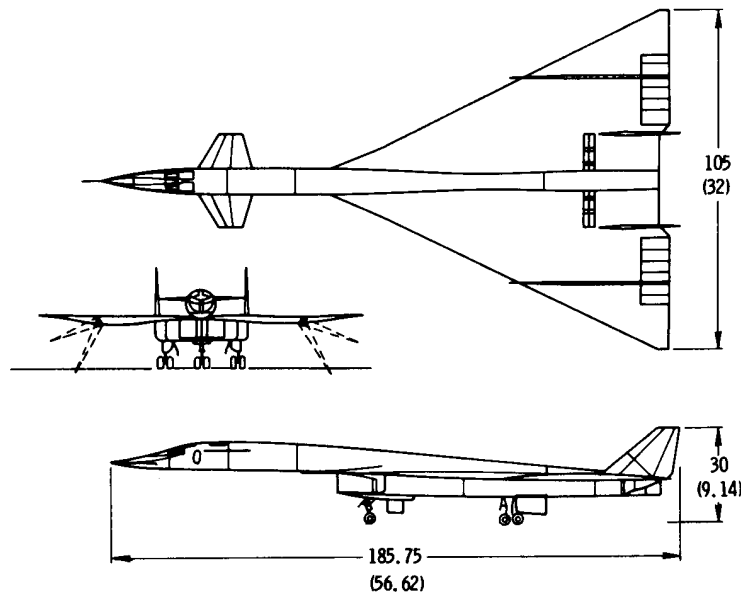


*Figure 1. Three-view drawing of the XB-70-1 airplane. Dimensions in feet (meters).*

The propulsion system consisted of two, two-dimensional inlets mounted side by side in a single nacelle under the center section of the wing. Each inlet supplied air to three YJ93-GE-3 afterburning turbojet engines. Each engine was in the 30,000-pound (133,000-newton), sea-level static-thrust class and had an 11-stage, axial-flow compressor, an annular combustion section, a two-stage turbine, and a variable-area converging-diverging exhaust nozzle.

## XB-70 INLET SYSTEM

The inlet was designed to operate in a mixed-compression mode as shown in figure 2; thus, the compression was accomplished partly through an external shock system and partly through an internal shock system, as indicated. At supersonic speeds less than Mach 2.0, the inlet operated only in an external compression (unstarted) mode with the terminal shock ahead of the inlet cowl. Each inlet was equipped with variable ramps and bypass doors, which could be positioned to maximize performance throughout the speed range, and a subsonic diffuser approximately 55 feet (16.76 meters) long that produced an equivalent conical angle of about 3°. The inlet boundary layer was controlled through a porous wall, boundary-layer-bleed system in the throat region.
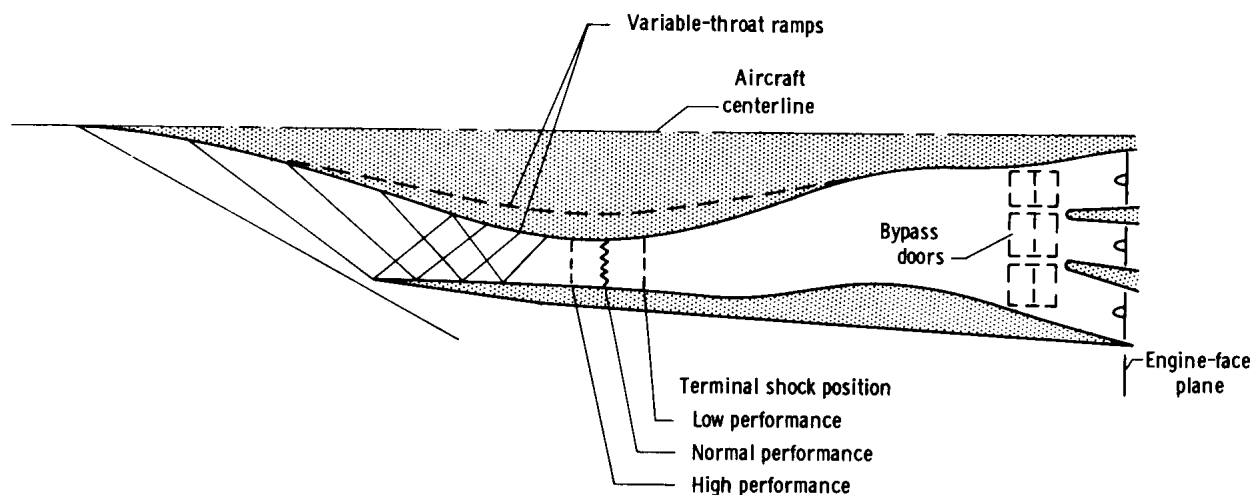


*Figure 2. Schematic drawing of the XB-70 air-induction inlet and shock-wave system. Top view, left side.*

The duct cross-sectional-area distribution is shown in figure 3 as a function of the distance relative to the geometric throat for a range of throat widths. In most instances, the geometric and aerodynamic inlet throats were not coincident because of boundary-layer effects.
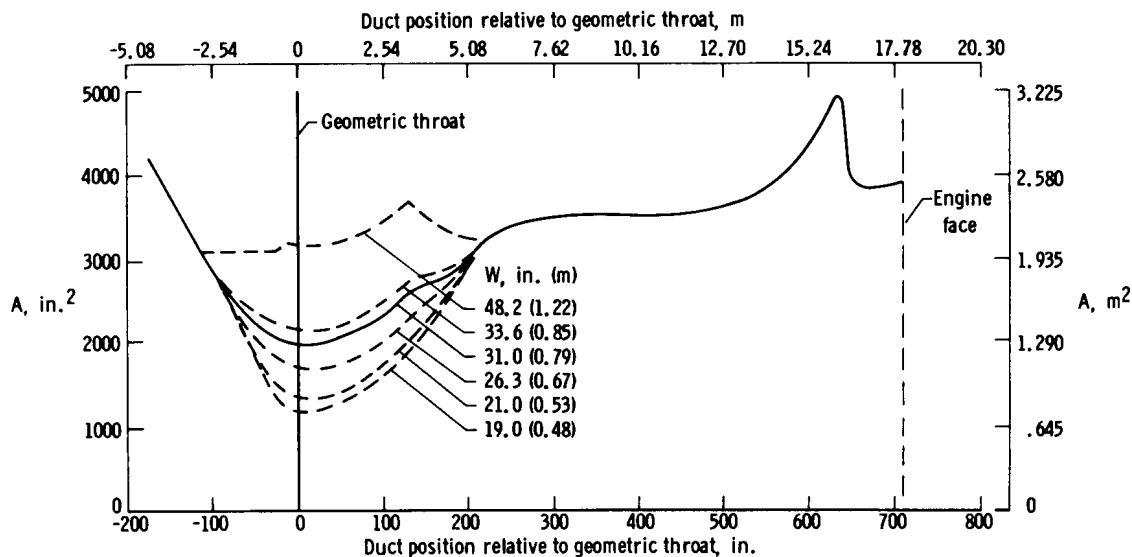
4

*Figure 3. XB-70 inlet cross-sectional area as a function of duct location and throat width.*

The left- and right-hand air-intake ducts each had six bypass doors on top, just forward of the engine face and exiting inboard of the leading edge of the vertical tails. These doors were used in conjunction with the controlled throat width to position the normal shock in each of the ducts and to match engine-airflow requirements.

The XB-70-1 airplane was equipped with a manual and semiautomatic air-induction control system; the system in the XB-70-2 airplane was automatic. All inlet simulations and flight data in this report are for the XB-70-1 inlet system operating in the manual mode, unless otherwise noted. The manual control of the propulsion system was a team effort, involving both the pilot and the copilot. The pilot normally controlled the engines, and the copilot controlled the air-induction system. In the manual mode of operation of the system, the copilot positioned both the throat and the bypass doors. The semiautomatic inlet control consisted of an automatic inlet control of the throat on a Mach number schedule along with the manual positioning of the bypass doors by the copilot. With the automatic inlet control system (XB-70-2), both the throat and the bypass doors were positioned automatically.

The inlet's performance was indicated to the copilot by a parameter known as inlet shock position ratio (SPR), which is defined as the ratio of a static pressure downstream of the inlet normal shock $p_s$ to a stagnation pressure upstream of the inlet normal shock $p_{impact}$.

It was advantageous to position the shock as near as possible to the aerodynamic throat (high SPR) where the entering Mach number would be a minimum, because shock strength and the total-pressure recovery are related to the Mach number directly upstream of the shock. However, for this type of inlet, the condition is unstable because small transients in airflow supply or demand can force the shock upstream of the throat. Once this occurs, mass, momentum, and energy relations require it to continue its upstream travel past the cowl lip. This is termed an unstart and is characterized by

5

large losses in total pressure through the shock system; the result is a total pressure at the engine face substantially below the free-stream level. In addition, other undesirable aerodynamic effects result, such as increased inlet drag, erratic aircraft motions, and a loss of thrust. Through careful manipulation of the movable throat and excess airflow bypass system, it is possible to maintain the normal shock slightly downstream of the aerodynamic throat such that stable operation with high total-pressure recovery is achieved. Simulation studies have shown the aerodynamic throat to be upstream of the geometric throat.

If the inlet normal shock is moved too far downstream (low SPR), other problems appear. Under such conditions the shock occurs at a higher Mach number and is consequently stronger. With the XB-70 terminal shock far downstream of the throat (supercritical), it was beyond the porous, boundary-layer-bleed region. Because the boundary layer was thicker downstream of the bleed region and the shock strength had increased, there was a significant shock—boundary-layer interaction producing airflow disturbances which could have had an adverse effect on engine operation and, in extreme cases, an engine stall could have resulted. Flight results from such supercritical operation are presented in references 7 and 8. Thus, it became desirable to decrease the SPR only enough to insure inlet stability yet not cause excessive performance degradation nor shock—boundary-layer interaction.

## SIMULATION MODEL AND PROCEDURE

The inlet model selected for the simulation is discussed in some detail in reference 2. As shown in figure 4, the analytical representation of the inlet is simple in concept. The model shown is for a started inlet and is considered to be analogous to a spring-mass system, in that it is divided into two volumes, Helmholtz and duct. The high-velocity air in the throat region (Helmholtz volume) is considered to be a mass of changing kinetic energy, whereas the low-velocity air behind it in the duct volume acts as a spring being compressed or expanded. The Helmholtz volume is defined such that its upstream face is the terminal normal shock and its downstream face is located so as to give simulation results that are comparable to wind-tunnel and flight data. Thus, the normal-shock acceleration is calculated through the application of instantaneous flow conditions to the Helmholtz volume. This acceleration is then integrated twice to obtain shock position versus time.
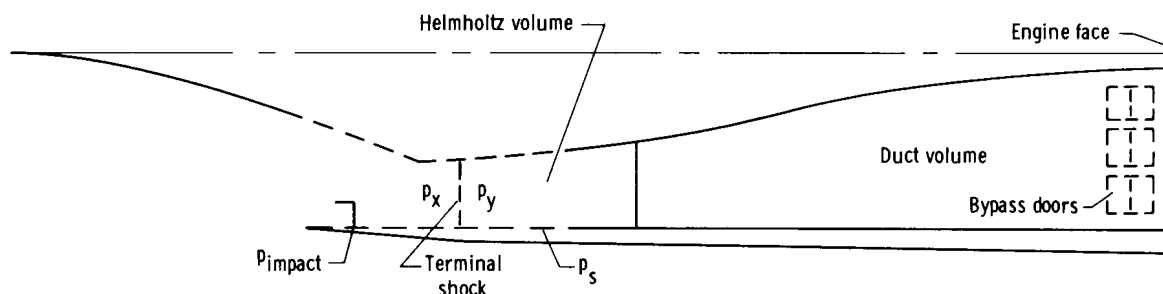
*Figure 4. Started-phase simulation model.*

The XB-70 digital simulation program can simulate five distinct modes of inlet operation. As in actual inlet operation, the program switches smoothly from one mode to another. The new mode is determined by switching logic, available in each subroutine, which continuously monitors the inlet's behavior. The ability to initiate switching is required so that the simulation may smoothly follow the inlet's reaction to either internal or external disturbances. When the appropriate subroutine has been selected, a special "initial conditions" subroutine computes the parameters needed for initiation of computation in the new phase.

The program has the capability of simulating started, unstarting, empty-fill (inlet buzz), subcritical, and hammershock modes of inlet operation. Although this report concentrates on started and unstarting phase simulations, an example is included of inlet buzz, a rapid emptying and refilling of the inlet accompanied by extreme boundary-layer separation and subsequent reattachment. A more common and considerably less severe model of inlet operation is that in which the expelled terminal shock stabilizes upstream of the cowl lip, producing all external shock compression and subsonic flow from the cowl lip to the engine face. This condition is known as subcritical operation. The need for the hammershock mode arises when duct outflow is suddenly reduced, such as during a compressor stall or rotor seizure. This causes a rapid increase in engine-face pressure followed by the propagation of a strong pressure transient upstream, thus the term "hammershock."

The simulations discussed in this report were obtained through the use of an IBM 7040/7094 direct couple system computer. Started and empty-fill phase computations were found to require 1.5 to 2.0 minutes of computer time per second of simulated inlet operation; unstarting calculations required about twice as much computer time.

Required input data for a typical simulation include aircraft angle of attack, angle of sideslip, and free-stream values of Mach number, static pressure, and static temperature. All of these parameters may be introduced as time-varying functions. This versatility coupled with the program's capability to handle time-varying inlet geometry enabled transients experienced in flight to be analyzed over a wide range of inlet performance levels.

Through application of the program, it was possible to determine the amount of performance decrease required to maintain started operation during typical free-stream disturbances such as horizontal temperature gradients and clear-air turbulence; conversely, in the absence of inlet changes, the likelihood of an unstart could be evaluated. The amount of total-pressure-recovery decrease from the normal operating level is termed the unstart margin. This margin is determined by decreasing the started inlet performance through successive increases in bypass-door opening until the inlet remains started through the transient.

In this study, the measured in-flight variation of the disturbing parameters was input to the computer as time-varying free-stream conditions. The response of the inlet at different performance levels was then analyzed by means of the simulation. Typically, the disturbance in terms of free-stream temperature, pressure, and Mach number together with angle of attack and sideslip changes was introduced about 1 to 2 seconds after the start of the simulation. This initial period allowed the inlet to seek a steady-state operating level before the transient was introduced.

Through these techniques, the unstart margins for the XB-70 inlet in the presence of both horizontal temperature gradients and clear-air turbulence were analyzed for a range of operating conditions.

## RESULTS

### Comparison of Simulated Unstart With Flight Data

One of the many planned unstarts in the XB-70 flight-test program demonstrated the capability of the simulation to predict flight results. This type of test was chosen because it successively used several of the inlet operating modes as the unstart progressed. The unstart was purposely induced by a gradual reduction in total bypass area, which caused a decrease in bypass airflow that moved the terminal shock upstream of the aerodynamic throat where it became unstable and continued upstream to the cowl lip (unstarted). Figure 5 compares engine-face total-pressure recovery and total temperature as a function of time for both the simulation and the flight results. Since the inlet's reaction to the bypass disturbance would be dependent on free-stream conditions, flight values of free-stream Mach number, static temperature, pressure, angle of sideslip, angle of attack, and a time history of the bypass disturbance were introduced to the simulation. Thus, the simulated inlet was presented with conditions, both steady state and dynamic, similar to those experienced by the full-scale inlet in flight.
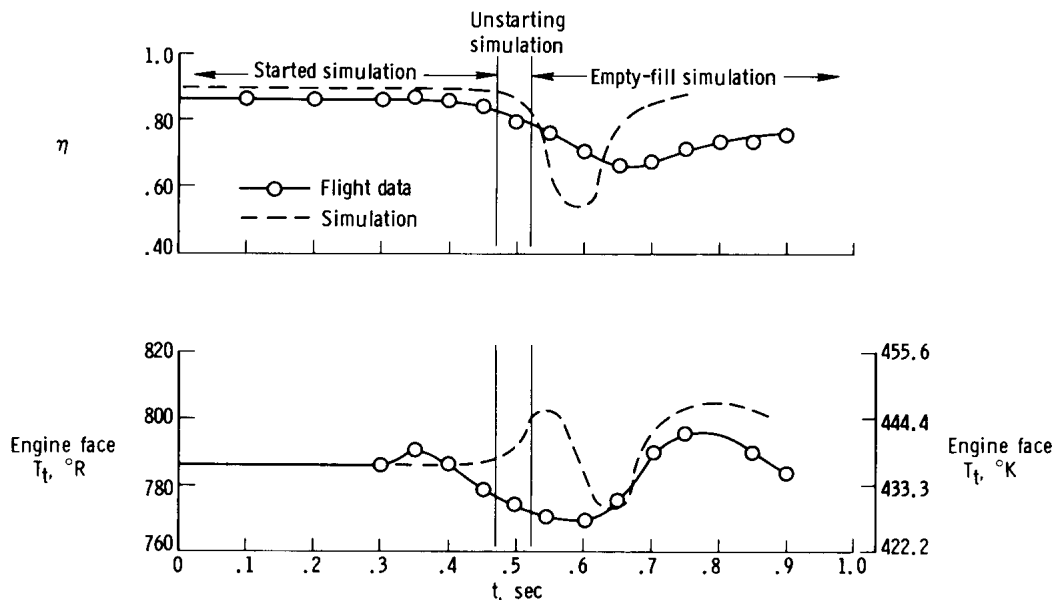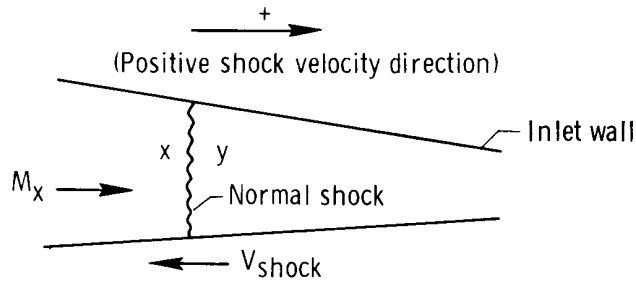


*Figure 5. Comparison of simulation and flight-test inlet data for a Mach 2.4 unstart induced by a reduction of bypass area.*

As seen in figure 5, the times of simulated and in-flight unstart are close, which indicates that the simulation can accurately predict whether a given disturbance will result in an inlet unstart. The initial pressure recovery of the simulation, however,

8

is 2 percent to 3 percent higher than that obtained from an area-weighted average of the in-flight measurements. (The high-response instrumentation system used for these inlet measurements is discussed in reference 7.) If the simulation is used to determine absolute recovery levels, it would appear that a judicious interpretation of the output would be required. In fact, it is recommended that where possible in the application of the simulation program, recovery deviations from some known reference level rather than absolute magnitudes be used. For this reason, all subsequent plots of inlet recovery are in terms of deviations from a steady-state value rather than absolute magnitudes.

Changes in total temperature were noted in both the flight and the simulation results shown in figure 5. It may not be obvious that total temperature changes during the unstarting transient, since total temperature is usually constant through a shock system. However, conservation of total temperature is required only for steady flow, and the unstart transient under study is obviously not steady. The time-dependent thermodynamic relations during the unstarting process, however, show that this total-temperature variation is directly related to terminal-shock velocity. As shown in the adjacent sketch, this velocity will be non-zero for the inlet unstarting, empty-fill, and hammershock processes. However, normal shock relations can be applied only if the shock is stationary. This condition can be accomplished by translating the coordinate system by the amount $V_{shock}$ such that it is stationary relative to the normal shock. If this is done, the Mach number of the incoming flow becomes

$$M_X' = M_X - \frac{V_{shock}}{c_X}$$

where $c_X$ is the local speed of sound immediately upstream of the moving shock, and shock velocities with the same direction as the incoming flow are considered positive.

Although an oversimplification, this effective Mach number $M_X'$ and the static temperature $T_{s_X}$ (which is independent of coordinate system) of the incoming air can now be used to obtain a total temperature $T_{t_X}$ relative to the stationary normal shock. It is this total temperature (now a function of shock velocity) that will be conserved across the normal shock, with proper regard for the relations between coordinate systems. The total temperature as measured at the engine face can now be determined. It thus becomes obvious that nonsteady engine-face total temperatures can be expected during any transient which produces appreciable terminal shock velocities. Reference 2 shows the details of the process and the flow charting of the computer solution. The more pertinent points of the discussion in reference 2 are included in the appendix of this report.

As shown in figure 5, the simulated total-temperature transient is of short duration, making a comparison with a flight-measured time history difficult because of the limitations of the aircraft temperature instrumentation. The discrete temperature points shown in the figure were obtained from a special probe immediately upstream of the engine face which could respond rapidly to changes in the total temperature of the engine airflow. However, the airborne instruments were not capable of precise magnitude determinations.

The significant points to be noted from the simulation total-temperature plots of figure 5 are the temperature rise during the unstart and the cyclic variation following the unstart, which is attributed to mild inlet buzz. Although the magnitudes and frequencies of the engine-face total-temperature variation as predicted by the simulation and as measured in flight differ, several similarities do exist between the two curves. The maximum peak-to-peak temperature change is approximately the same for both curves and both exhibit a total-temperature rise followed by a decrease and another rise, as would be expected during a buzz cycle. Since the total-temperature probe used in flight was only a prototype design, further refinements would be required before more detailed comparisons between the two curves would be justified. Also, since the instantaneous engine-face total temperature is a function of shock velocity and the Mach number $M_x$ of the air entering the shock, total-temperature distortion across the engine face could conceivably result, since $M_x$ will likely be nonuniform across the inlet duct. These facts should not be overlooked when stall tolerance problems are studied.

In general, the simulation results shown in figure 5 indicate reasonable agreement between flight data and the started and unstarting phase calculations, which are based on a rigorous analytical foundation (ref. 2). This comparison indicates that the models used for the started and unstarting phase simulations are, indeed, valid representations of the processes as they occurred in flight. In the empty-fill phase, however, the governing mechanism is boundary-layer separation, as illustrated in figure 6. The simulation defines the separated boundary layer by constants such as boundary-layer height, reattachment point, and reattachment pressure ratio. These parameters were based on the results of wind-tunnel testing and were characterized by their non-repeatability under similar test conditions. Thus, it is not surprising that the correlations between the empty-fill simulation and flight data are not as good as similar correlations for the started and unstarting phases. These comparisons indicate the need for further refinements in the empty-fill model used.
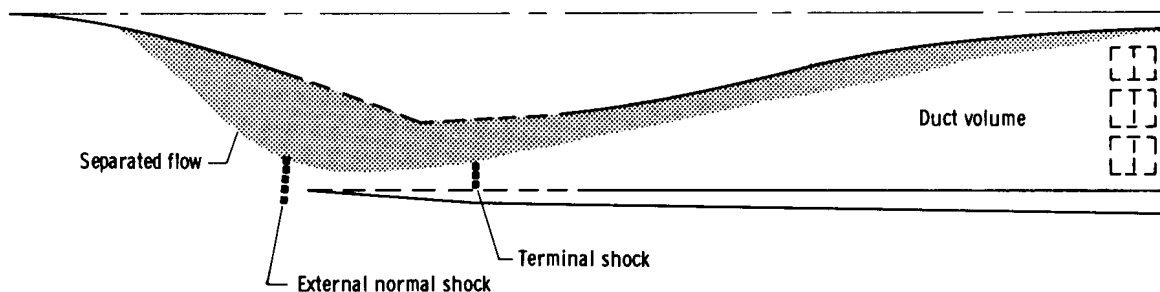


*Figure 6. Empty-fill-phase simulation model.*

## Effect of Free-Stream Disturbances

If inlet stability is to be maintained, careful attention must also be paid to external transients such as clear-air turbulence or free-stream temperature gradients. Disturbances of both types were encountered during the XB-70 flight program and were of sufficient intensity to require adjustments to the air-induction system to insure stable operation through the transient.

Free-stream temperature gradient. – An example of the effect of a horizontal static-temperature gradient on the started XB-70 inlet is shown in the 2-minute segment of actual flight data in figure 7. It is significant that for this interval, no appreciable turbulence was observed. The effect on inlet performance of the free-stream total
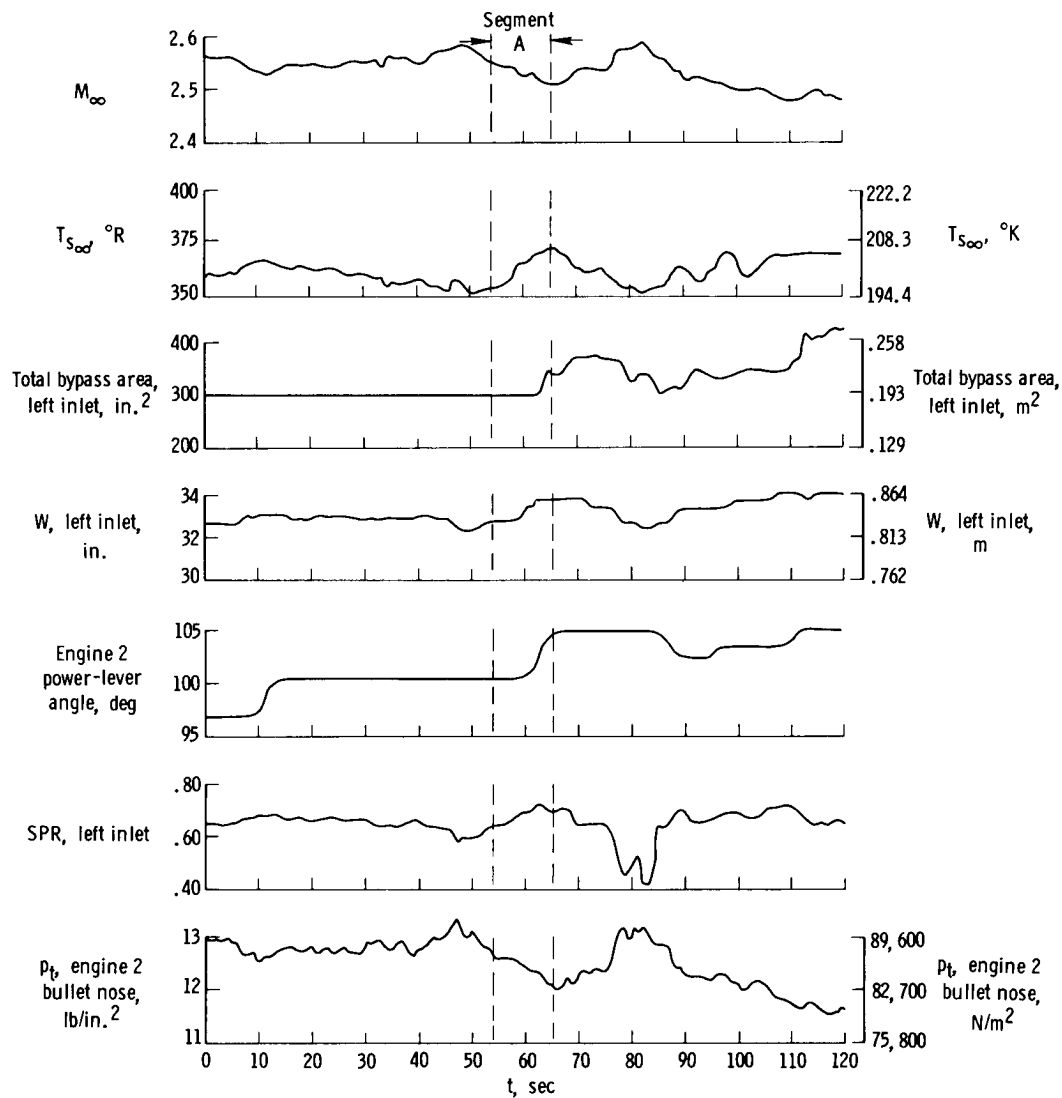


Figure 7. Free-stream temperature gradient and its effect on the XB-70-1 propulsion system in flight at M = 2.5, h = 60,000 feet (18,300 meters).

temperature and Mach number variations and responses of the pilot and copilot are indicated by such quantities as engine-face total pressure, throat width, and bypass area. The entire 2-minute interval is of a transient nature, with some of the steepest gradients in free-stream conditions occurring within the intervals from 54 to 60 seconds and 90 to 95 seconds. The first 50 seconds of the transient contained gradual free-stream temperature variations which required a slight increase in power at about $t = 10$ seconds to compensate for the preceding drop in Mach number. No changes in throat width or total bypass area were made during this interval. At approximately 54 seconds, however, the free-stream static temperature started to rise rapidly, causing Mach number to decrease and the shock pressure ratio to rise. The copilot, realizing that the SPR was increasing very close to the point of unstart, opened the bypass doors. At the same time, the pilot noted the Mach number drop and attributed it to a free-stream velocity decrease, so he advanced the power lever to obtain additional thrust.

As shown in figure 7, the inlet total pressure measured at the bullet nose of engine 2 was high when the SPR was low and vice versa, which is contrary to what would be expected. However, it should be noted that total pressure closely follows the free-stream Mach number; thus, it becomes evident that Mach number is the predominant factor. An additional point to be noted is the wide excursions in SPR from 70 to 85 seconds. Such fluctuations are representative of the inlet's sensitivity to transient disturbances when operating in a low-performance mode. This is clearly an undesirable operating region both from a performance and an inlet stability viewpoint.

After this temperature gradient was encountered, the question arose whether an unstart would have occurred had the copilot not altered the inlet geometry. In addition, the precise amount of corrective action or performance degradation required for the inlet to remain started was uncertain. Further insight into the effect of this segment of the overall transient on the started inlet at various initial pressure-recovery levels without pilot intervention was achieved through the use of the XB-70 inlet simulation. The results of these simulations are shown in figure 8 as time histories of shock position and recovery change for a range of initial inlet performance levels. The simulations starting at $t = 1$ second in figure 8 represent the reaction of the inlet to the disturbance beginning at $t = 54$ seconds in figure 7 (segment A). For all levels investigated, the free-stream transient resulted in a gradual movement of the terminal shock toward the throat. At the lower performance levels, represented by runs D to F, this upstream shock movement resulted in a final shock position still substantially downstream of the geometric throat. At the higher performance levels of runs B and C, the shock stabilized close to the throat; finally, with the initial performance level of run A, the free-stream transient moved the shock upstream of the aerodynamic throat, causing an inlet unstart as shown by the rapid recovery dropoff.

Run A represents inlet conditions encountered in flight and clearly indicates that the inlet would have unstarted if the copilot had not initiated preventive measures. From the results of runs B to F the total-pressure-recovery decrease needed to maintain started operation throughout the transient can be determined. Figure 8 indicates that a recovery decrease to the levels of runs C or D (reductions of 0.6 to 0.8 percent) would have insured started operation.

In addition, it should be noted that, although the interval chosen for detailed analysis represented the maximum change in free-stream static temperature during
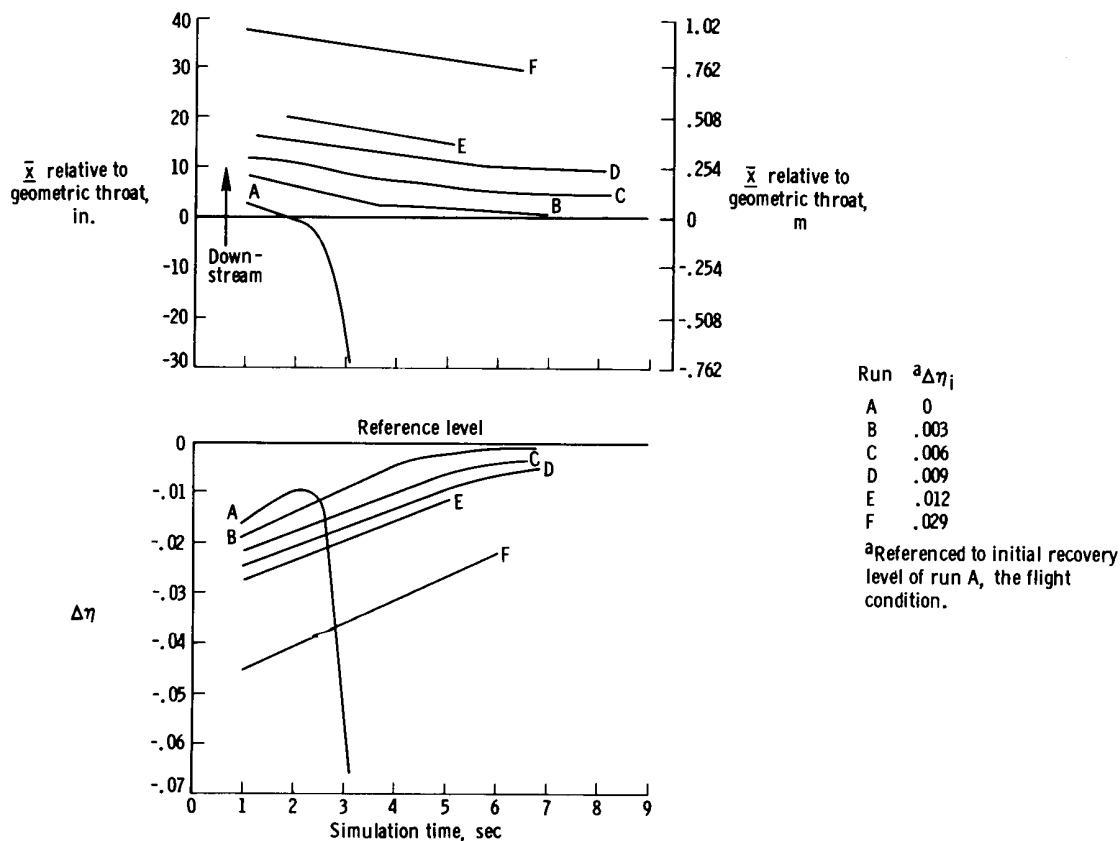
**Run** $^a\Delta\eta_i$

A    0
B    .003
C    .006
D    .009
E    .012
F    .029

$^a$Referenced to initial recovery
level of run A, the flight
condition.

*Figure 8. Simulated effect on inlet performance of free-stream temperature gradient shown in time segment A of figure 7. M = 2.5; h = 60,000 feet (18,300 meters).*

the 2-minute transient of figure 7, it is possible that the rate rather than the absolute magnitude of the change would be the controlling factor; thus, the rise in temperature from t = 84 to 86 seconds should be considered. As indicated by references 9 and 10, disturbances similar to those discussed in this report have been measured as part of several atmospheric-turbulence studies and are considered to be of importance in the supersonic-transport program. In any event, the experience gained during the study of this type of free-stream disturbance indicates that the disturbances are a factor which must be considered in future mixed-compression-inlet design and further indicates the applicability of a digital inlet simulation to such studies.

Turbulence. — In the transient shown in figure 7, the induced aircraft motions were not large enough to influence inlet performance or stability; however, aircraft dynamics during turbulence can be a significant part of the inlet disturbance and should be considered. The XB-70 airplane encountered areas of clear-air turbulence on several flights (refs. 10 and 11) in which the resultant aircraft motions significantly affected the performance of the started inlet. To maintain started operation within such turbulence, either an inlet control system must adjust the inlet geometry rapidly or the inlet pressure recovery level must be reduced manually or automatically by an inlet control system.

13

Since representative turbulence data were available from several XB-70 flights on both the free-stream conditions and the aircraft's reaction to the disturbances, their effect on inlet operation over a range of operating levels could be readily assessed through the use of the digital inlet simulation.

A typical 2-minute time history of airplane response and free-stream environment experienced by the XB-70-2 airplane in moderate turbulence at a free-stream Mach number of 2.5 and an altitude of 60,000 feet (18,300 meters) is presented in figure 9.
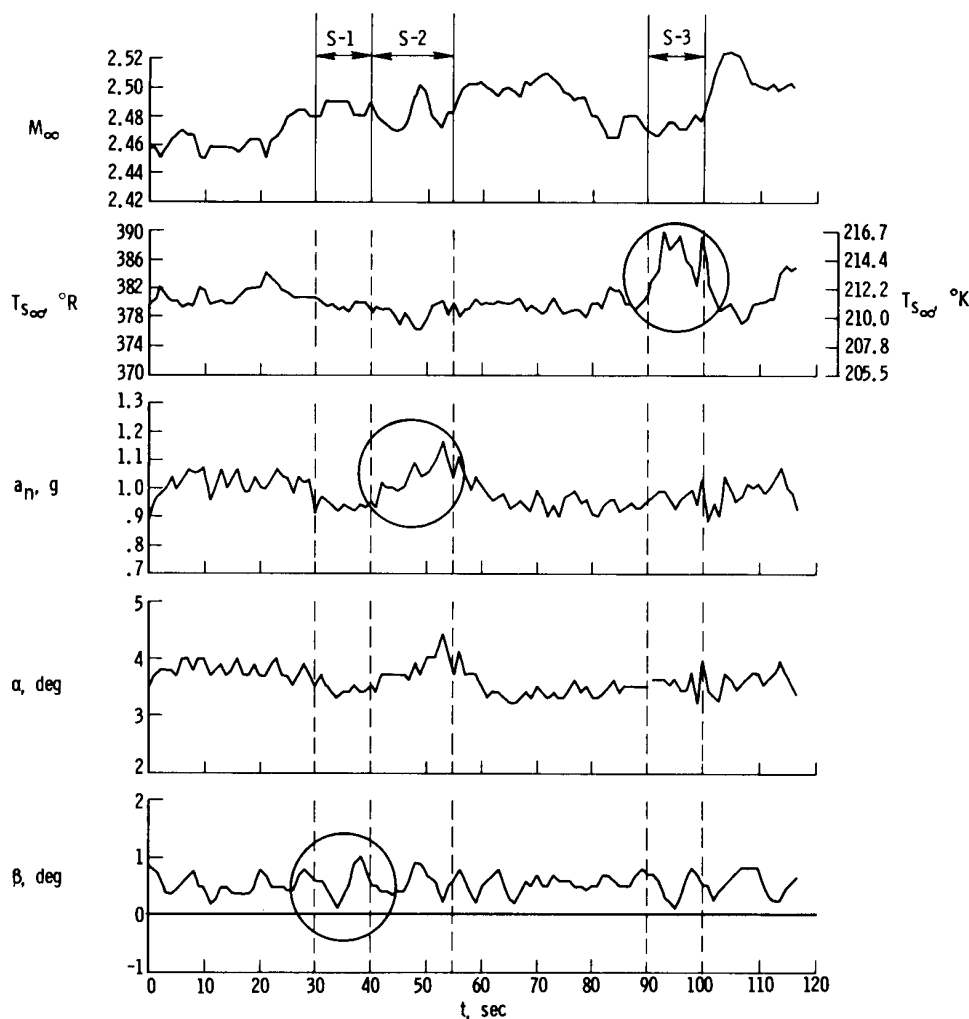


Figure 9. Effect of free-stream turbulence on the XB-70-2 in flight at M = 2.5, h = 60,000 feet (18,300 meters).

The reaction of the automatic inlet control system of the airplane to these 2 minutes of turbulence is shown in figure 10 (solid lines) by the positions of the bypass main and trim doors, which were controlled as a function of SPR by the automatic control system. In the absence of the automatic control system, continuous started operation would have required that the terminal shock be positioned farther downstream of the throat, with a resultant decrease in inlet performance. For comparison, a trace (dashed lines) of
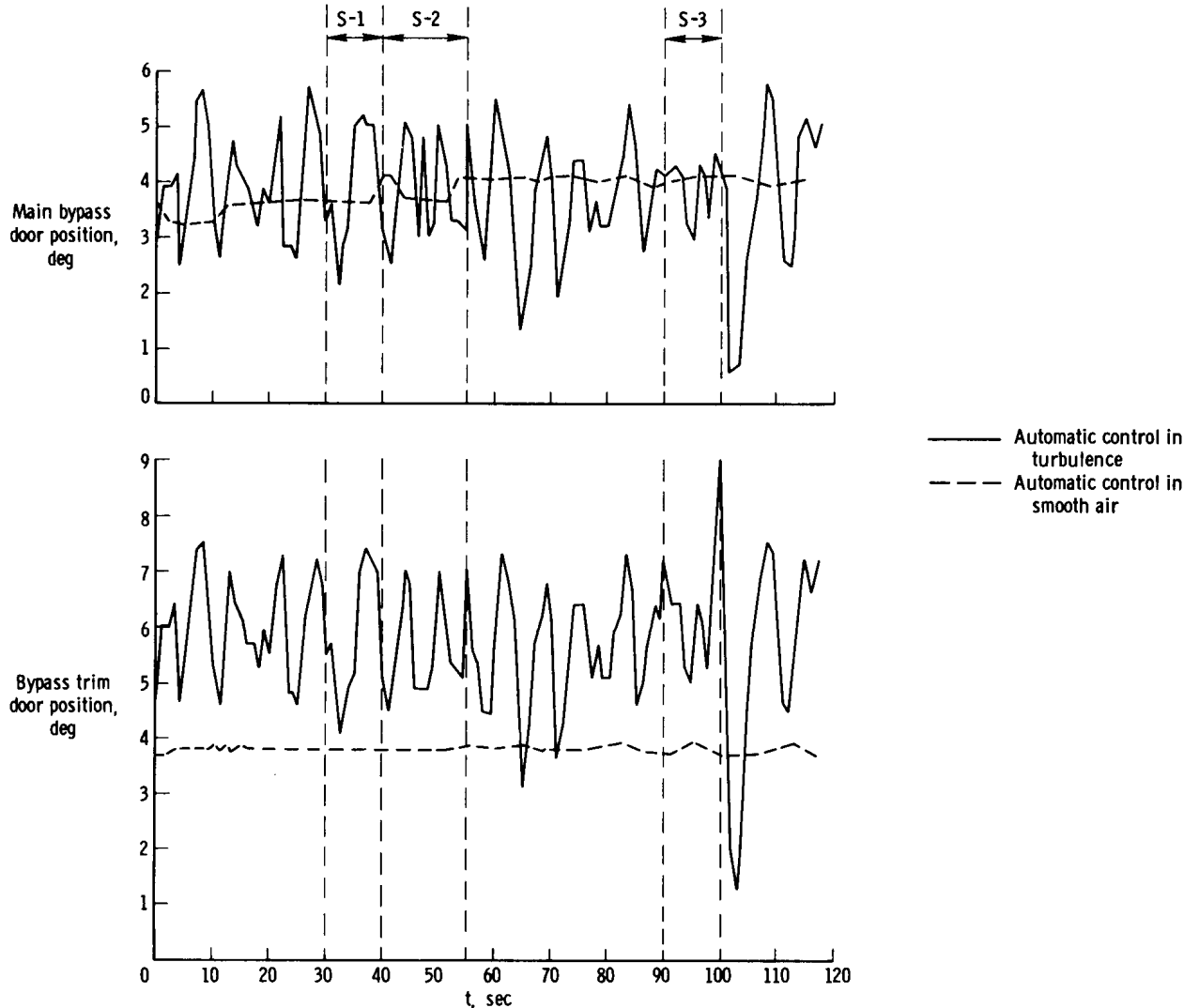
14

*Figure 10. Typical XB-70-2 bypass-door positions during flight in free-stream turbulence and in smooth air with the automatic inlet control system operating.*

the automatic inlet control bypass door positions for XB-70-2 flight at the same Mach number and altitude through smooth air is included in the figure. Thus, it is evident that the automatic control system responds very rapidly to (turbulent) free-stream conditions.

The digital inlet simulation program was used to determine the reaction of the inlet to this encounter with turbulence over a range of initial geometry settings (bypass areas) in the absence of an automatic inlet control system. Several turbulence samples (S-1, S-2, and S-3) were selected from the flight data of figure 9 for use as free-stream inlet disturbances. These samples were chosen on the basis of the following criteria: interval S-1, because of the angle-of-sideslip variations; interval S-2, because of high normal-acceleration changes; and interval S-3, because it contained rapid free-stream static-temperature fluctuations. Although the data samples did

15

appear to be dominated by the specific parameters discussed, it was realized at the time of selection that the effects of the parameters could very well be masked or severely altered through interaction with the other time-varying quantities. The digital-simulation approach adapts well to the handling of several such time-varying conditions simultaneously.

Several simulations were then completed over a range of initial inlet performance levels for each of the three turbulence samples. The resulting upstream and down-stream shock movements for the three disturbances chosen are summarized in figures 11 to 14.

From an inlet viewpoint, the turbulence sample chosen because of the associated high aircraft normal accelerations (S-2) proved to be less severe than either of the other two samples, producing a maximum recovery fluctuation of 1 percent as seen in figure 11.
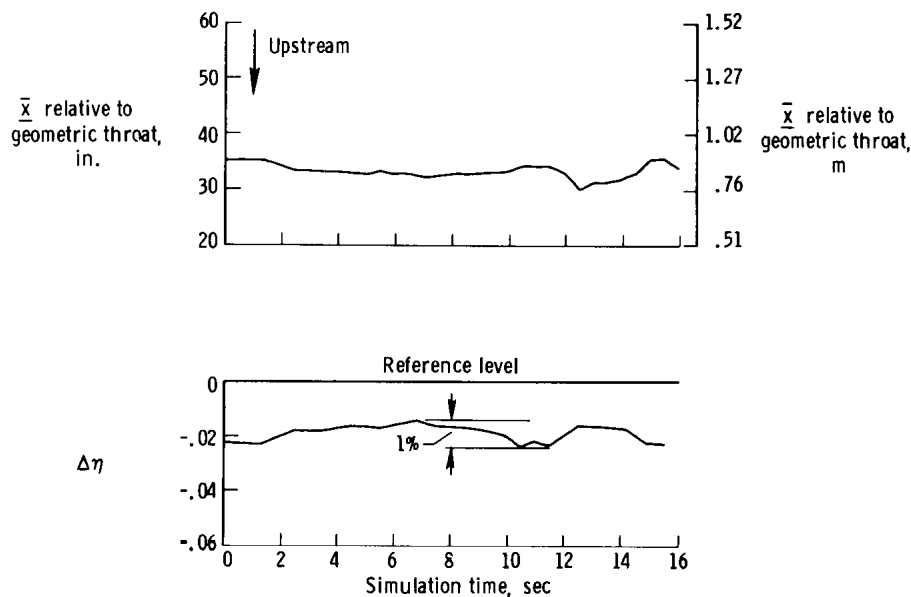


Figure 11. Simulated effect on total-pressure recovery and inlet terminal-shock position of free-stream turbulence producing significant aircraft normal accelerations (sample S-2, fig. 9). M = 2.5; h = 60,000 feet (18,300 meters).

Figure 12 summarizes the response of the inlet simulation to the data sample selected on the basis of free-stream static-temperature fluctuations (S-3) and shows an area of forward shock movement from t = 7.5 seconds to 11.5 seconds. This illustrates the possibility of inlet unstart associated with free-stream turbulence. The figure contains a family of curves (runs A to E) that indicates the response to the free-stream disturbance of the terminal inlet shock in terms of shock movement and associated total-pressure-recovery variation for a range of initial inlet performance levels. The figure further indicates that, for the range of performance levels repre-sented, a change in the initial shock position prior to the start of the transient simply causes a translation of the shock-position curve while leaving the shape of the curve essentially unaltered. This in turn causes a similar shift in the level of the recovery curve with no significant change in its shape.
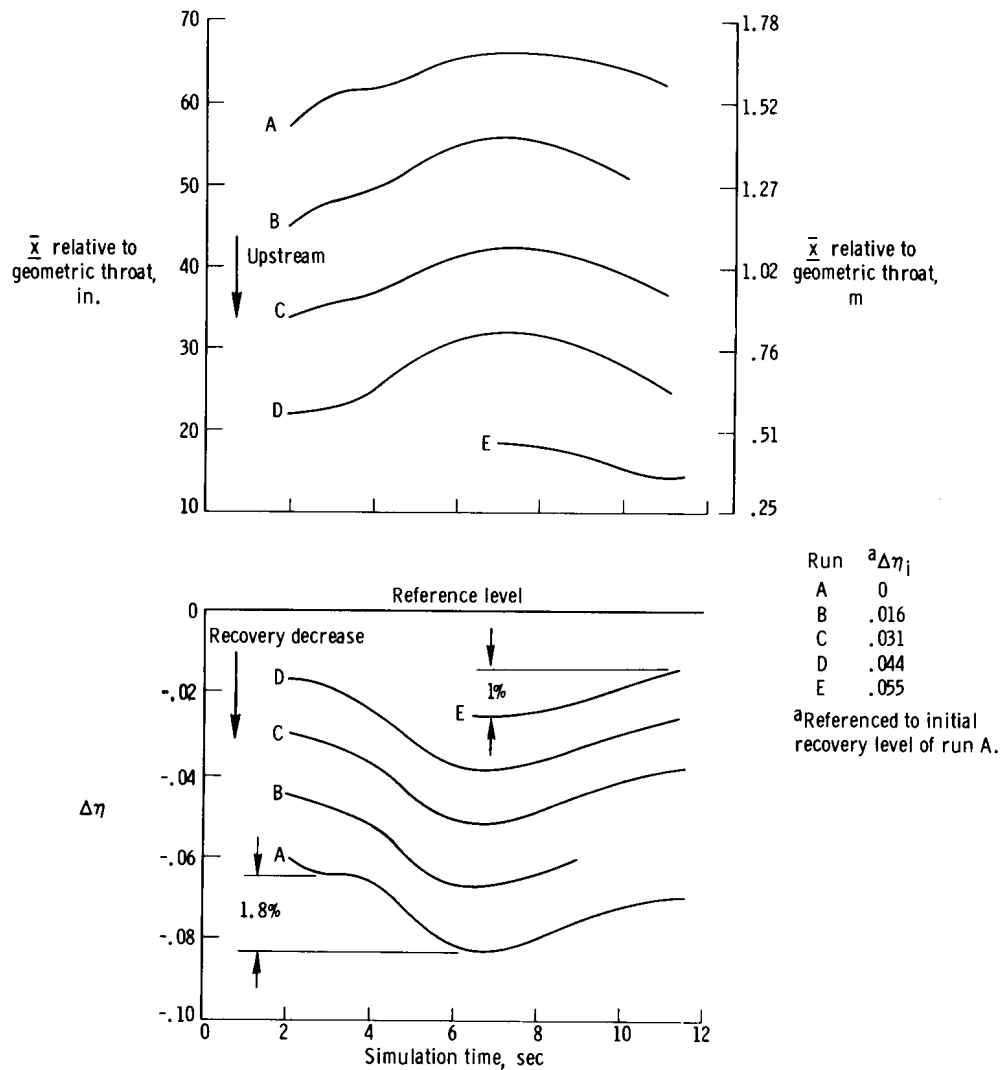
16

*Figure 12. Simulated effect on total-pressure recovery and inlet terminal-shock position of free-stream turbulence containing significant free-stream static-temperature fluctuations (sample S-3, fig. 9). M = 2.5; h = 60,000 feet (18,300 meters).*

An approximately linear relationship is indicated in figure 13 between initial shock position and inlet total-pressure recovery for the performance range represented by figure 12. This relationship is attributed to the fact that for the inlet throat width used in this Mach number range (approximately 31 in. (0.79 m)), the duct cross-sectional-area versus distance relationship is approximately linear. (See fig. 3.) Since the oblique-shock losses upstream of the aerodynamic throat and the subsonic-diffuser losses are approximately constant through the transient, any recovery changes must be due primarily to the changes in terminal-shock strength. Furthermore, the total-pressure ratio across a normal shock is linearly related to the area ratio $A_x/A^*$ for

throat Mach numbers from 1.1 to 2.0, as shown by the insert in figure 13. For this study, the Mach number immediately upstream of the terminal inlet shock falls within this range, and, since $p_{t_x}$ and $A^*$ are assumed to be constant, the change in total pressure is linearly related to duct cross-sectional area or terminal-shock position,
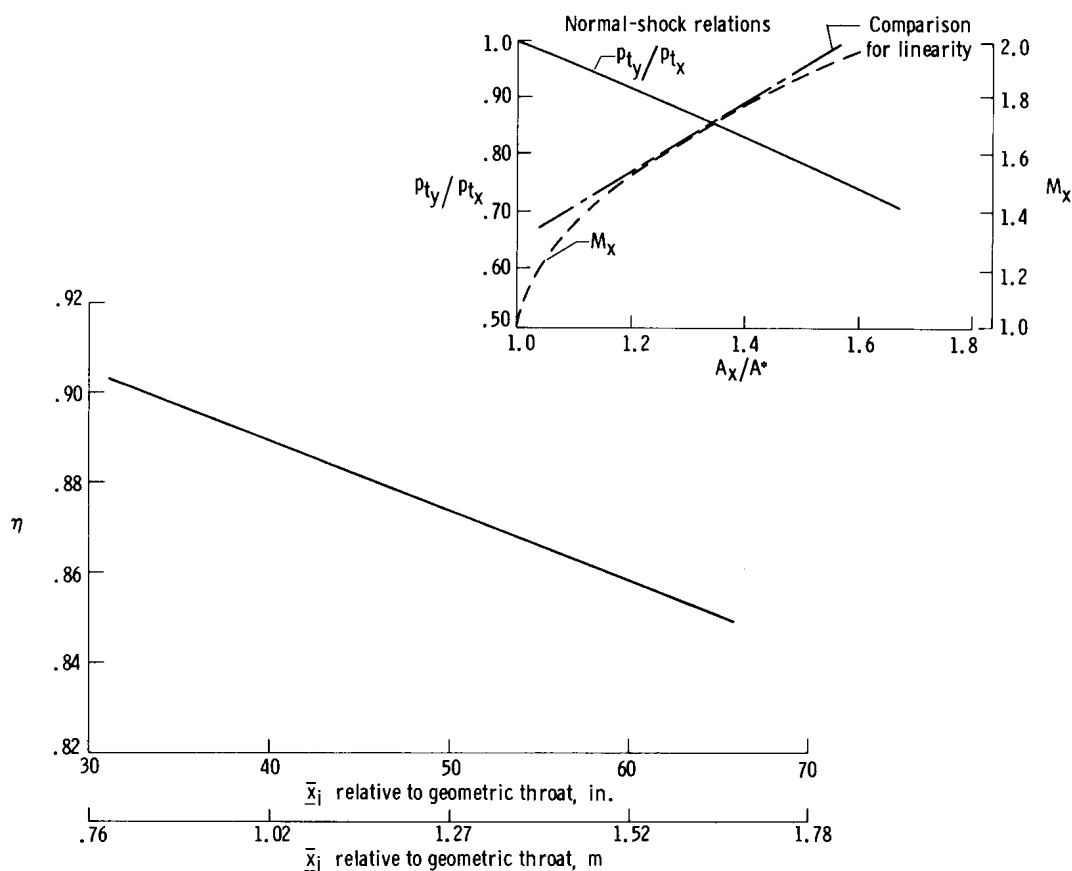
17

*Figure 13. Simulated initial terminal-shock position versus initial simulation recovery. M = 2.5; h = 60,000 feet (18,300 meters).*

as the simulation has shown. It is expected that this linear relationship ceases, however, in the immediate vicinity of the throat, since the variation of cross-sectional area with longitudinal position in the duct is nonlinear. In addition, the effects of boundary-layer bleed within the inlet have been ignored in this discussion.

Figure 12 further indicates that recovery changes of 1 percent to 1.8 percent could be caused by this turbulence sample. For economical operation, such variations in performance are probably significant. It should be noted that recovery changes in figure 12 and all succeeding figures will be related to some arbitrary reference level, since, as previously discussed, the absolute magnitude of the simulation-predicted recoveries may be questionable.

Similar inlet behavior for the sideslip-dominated turbulence sample (S-1) is shown in figure 14, with recovery variations of 2 percent to 2.3 percent experienced. Since the segment of the sideslip-dominated sample (S-1) in figure 14 resulted in a 2.3-percent recovery increase (relative to t = 6 sec), this segment presented the greatest possibility of free-stream turbulence-induced unstart and was extracted for more complete study. A two-phase (starting and unstarting) simulation was used to
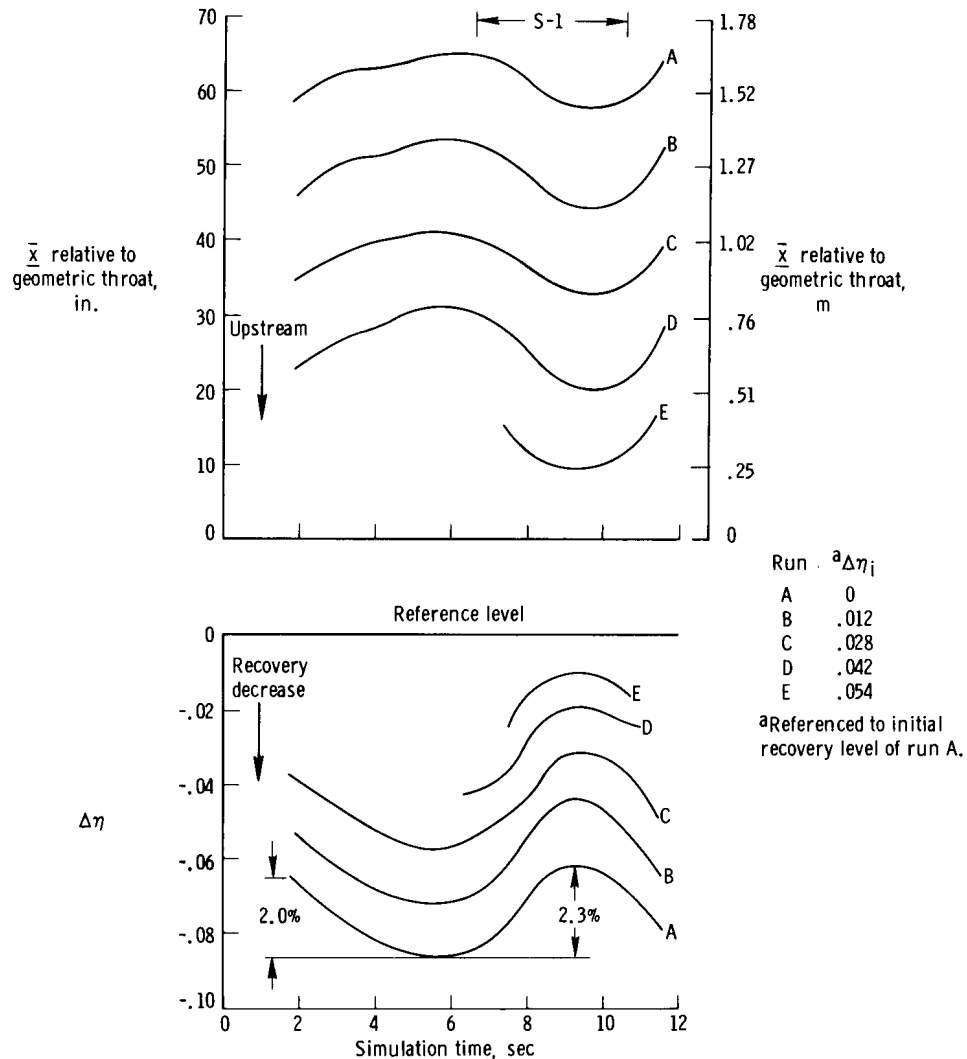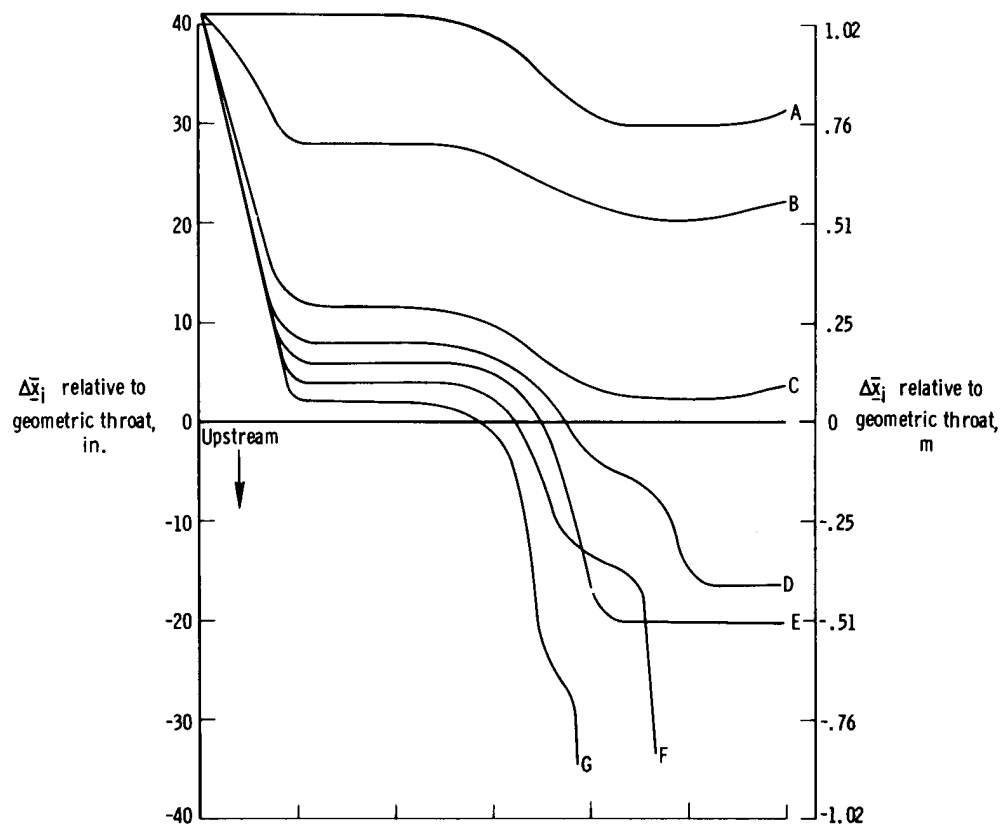
Figure 14. Simulated effect on total-pressure recovery and inlet terminal-shock position of free-stream turbulence producing significant sideslip fluctuations. M = 2.5; h = 60,000 feet (18,300 meters).

establish the unstart margin required to maintain started operation throughout the transient. The results of this investigation are shown in figure 15.

As shown by the cross-hatched region in figure 15, it is difficult to establish precisely the maximum attainable inlet recovery, since the severity of the free-stream disturbance is dependent on the relationship between terminal-shock dynamics and the interaction of several time-varying free-stream quantities. Also, notice that the simulation predicts that a started inlet will be maintained through the turbulence for runs A to E. In these runs the terminal shock has stabilized downstream of the aerodynamic throat, which for runs D and E occurs slightly ahead of 17 inches (43.18 centimeters) and 20 inches (50.80 centimeters), respectively, upstream of the geometric throat. Thus, the data of figure 15 show that a recovery level of at least 1 percent below the maximum (and, to be conservative, probably close to 1.5 percent) would be required prior to the encounter of clear-air turbulence.

19

40

30

20

10

$\Delta \bar{x}_i$ relative to
geometric throat,
in.

0

Upstream

-10

-20

-30

-40

1.02

.76 ── A

.51 ── B

.25

$\Delta \bar{x}_i$ relative to
geometric throat,
m

0

-.25

-.51 ── D
── E

-.76

G    F

-1.02

A
B
C
C

| Run | $^a\Delta\eta_i$ |
|-----|-----------|
| A | 0 |
| B | .012 |
| C | .025 |
| D | .029 |
| E | .030 |
| F | .031 |
| G | .032 |

[a]Referenced to initial
recovery level of run A.

Region of maximum recovery

0

1.5%

1.0%

-.01    G    F

E ── D

C

-.02

$\Delta\eta$

-.03

$\Delta\eta_i$ for run
B = 1.2%

-.04

Recovery
decrease

-.05

C

D
E

B

A

G    F
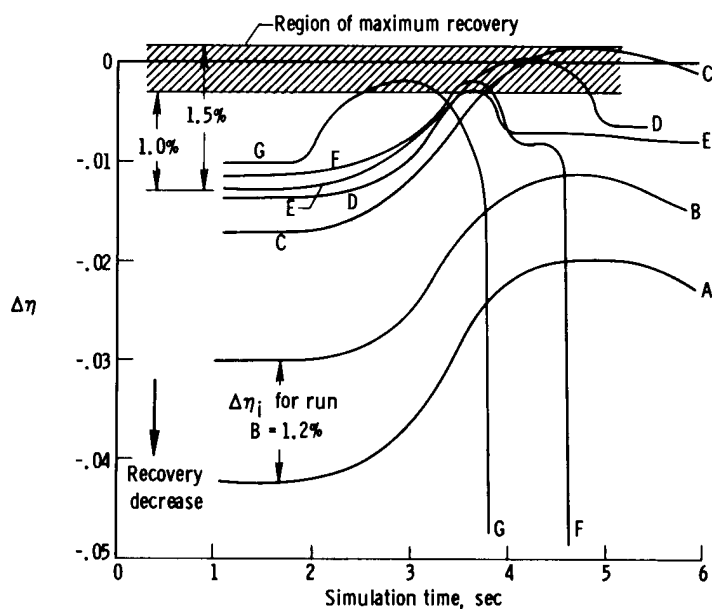
0    1    2    3    4    5    6
Simulation time, sec

Figure 15. Simulation-determined unstart margins for free-stream turbulence experienced in
flight at M = 2.5, h = 60,000 feet (18,300 meters).

20

Figure 16 illustrates the complex and unpredictable nature of the reaction of the XB-70 inlet to free-stream turbulence disturbances which might be encountered in flight and shows that no two transients affect the inlet in the same manner. This is a plot of terminal-shock movement for four separate simulation runs, with the terminal shock originally positioned at approximately the same duct location and subsequently perturbed by the different turbulence samples used previously (S-1 to S-3, fig. 9). The disturbances for runs A and C were two different static-temperature transients (one increasing and the other decreasing) extracted from sample S-3, for run B from the acceleration sample S-2, and for run D from the sideslip sample S-1. A comparison of the shock movements for these four disturbances demonstrates the range of turbulence effects and the markedly different inlet reactions. The differences are apparently due to the relative levels of the M, $T_s$, $\alpha$, and $\beta$ variations within the

different samples as well as the phase relationships between these same parameters within a given turbulence sample. The sample with predominantly temperature changes was found to be nearly as significant as the severe turbulence cases in terms of necessary inlet recovery margin.
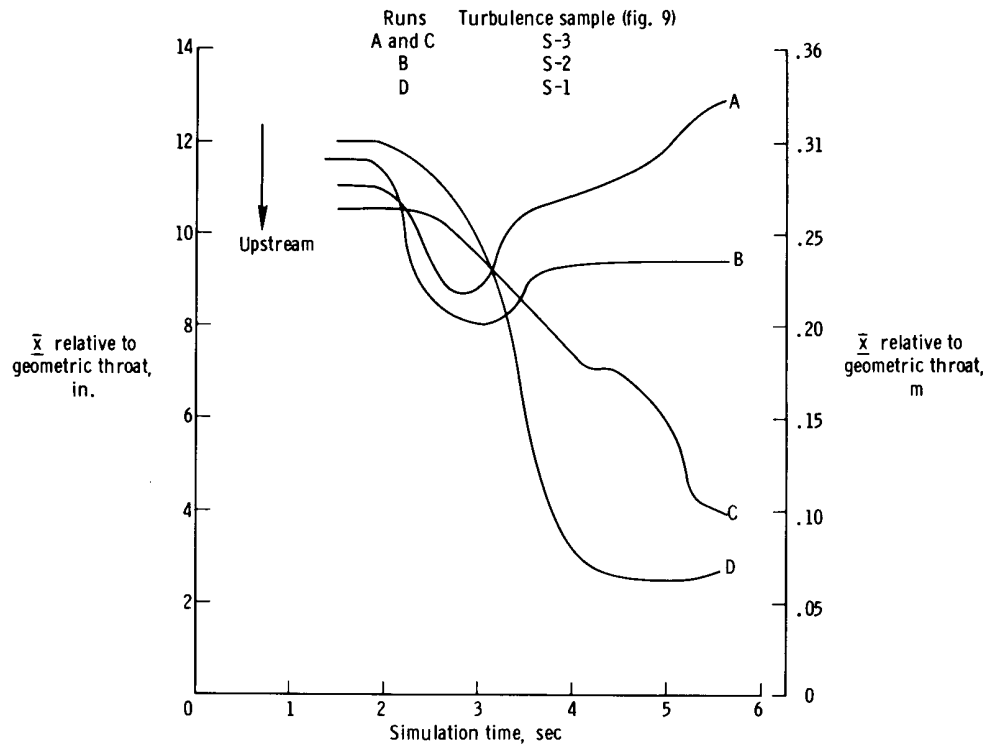


*Figure 16. Comparison of simulated response of terminal shock to three distinct turbulence samples.*
*M = 2.5; h = 60,000 feet (18,300 meters).*

It should be noted, however, that the effects of clear-air turbulence on the performance of a mixed-compression inlet system can be significant and should be considered in the design of an inlet control system and in the determination of the steady-state operating level of the inlet.

# CONCLUSIONS

An analysis was made of the capability of a digital inlet simulation program to predict the performance of the started XB-70 inlet system and the dynamic aspects of an inlet unstart at Mach numbers from 2.4 to 2.6. The simulations and flight data discussed in this report were for the XB-70 aircraft. Thus, although some of the information is of a general nature, care should be used in extending the conclusions drawn from the analysis to other inlet systems. The investigation showed that:

1. A digital simulation technique incorporating multiple input capability was useful in describing the behavior of a complex propulsion system under a multiplicity of dynamic conditions.

2. Concepts used to simulate started and unstarting phases provided results which compared favorably with flight data. However, comparisons between empty-fill simulations and flight data indicated the need for additional work on the boundary-layer model used.

3. In the absence of an automatic inlet control system, moderate free-stream turbulence can produce engine-face total-pressure-recovery transients of up to 2.3 percent from normal operating levels. With the inlet operating at a high performance level, these same transients would require that the inlet be operated 1 percent to 1.5 percent below maximum recovery if started operation were to be maintained through the transient.

4. The inlet terminal-shock movements associated with inlet unstarting and empty-fill processes could result in appreciable time-varying engine-face total temperatures and possible engine-face total-temperature distortions.

5. The effects of free-stream turbulence and temperature gradients should be considered in the design of inlet control systems. Variations in atmospheric temperature were found to be nearly as significant as severe turbulence for a mixed-compression inlet.

Flight Research Center,
   National Aeronautics and Space Administration,
      Edwards, Calif., February 13, 1970.

# APPENDIX

## TOTAL-TEMPERATURE CHANGE DURING AN UNSTART

As discussed in the section on Comparison of Simulated Unstart With Flight Data, transient fluctuations in total temperature were measured by high-response probes at the engine face of the XB-70 airplane during an unstart. Although the cause of such changes may not be immediately apparent, a detailed discussion of the probable mechanism that causes the changes is included in reference 2. To clarify some of the flight data presented in this report, the more pertinent points of the engine-face total-temperature calculations presented in reference 2 are summarized in the following discussion.

As in the unstarting phase of the simulation program, the inlet is considered to be represented by one "lumped volume" whose upstream face is coincident with the terminal inlet normal shock. Such a configuration is representative of an unstart induced by insufficient airflow demand and has been found to adequately represent the inlet during this transient. A model of such a configuration is shown in the following sketch:
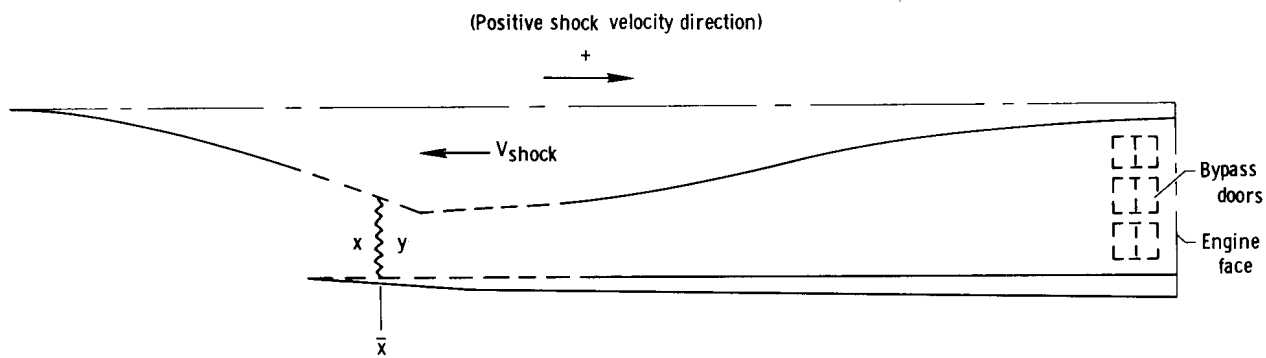


As shown, conditions upstream of the normal shock are designated by the subscript x, those immediately downstream by y, and those in the duct volume itself by d.

For steady-state operation with the terminal inlet shock stationary, the duct volume will be at some total temperature $T_{t_{d_i}}$, constant throughout, such that

$$T_{t_{d_i}} = T_{t_{y_i}} \tag{1}$$

During the unstarting phase, the terminal shock moves upstream so that its instantaneous upstream Mach number as denoted by the prime superscript can be written as

$$M'_x = M_x - \frac{d\bar{x}/dt}{c_x} \tag{2}$$

where $\bar{x}$ denotes shock position, t, time, and $c_x$, local speed of sound.

By knowing $M_x'$, $T_{s_x}$ and $T_{s_y}$ can be calculated from normal-shock relations, since

$$T_{s_y} = f\left(T_{s_x}, M_x'\right) \tag{3}$$

and by knowing $M_x'$, $M_y'$ can be obtained from these same relations, as follows:

$$M_y' = g(M_x') \tag{4}$$

From this expression, the downstream Mach number relative to the duct is calculated from the equation

$$M_y = M_y' + \frac{d\bar{x}/dt}{c_y} \tag{5}$$

and the downstream total temperature relative to the duct, from the equation

$$T_{t_y} = f\left(T_{s_y}, M_y\right) \tag{6}$$

Since this is a transient process, the duct total temperature will be somewhere between the value immediately downstream of the terminal shock $T_{t_y}$ and that of the remainder of the duct volume $T_{t_{d_i}}$. The duct-volume total temperature is considered to adjust to the varying $T_{t_y}$ through the relation

$$T_{t_d} = T_{t_{d_i}} + \int_i^t \left(\frac{dT_{t_d}}{dt}\right) dt \tag{7}$$

The rate of change of duct-volume total temperature $dT_{t_d}/dt$ is approximated by the relation

$$\frac{dT_{t_d}}{dt} = \frac{\left(T_{t_y} - T_{t_d}\right)}{\Delta t}$$
$$= \frac{\text{Total-temperature change}}{\text{Change in characteristic time}} \tag{8}$$

where the characteristic time is defined as

$$t = \frac{\text{Mass air in duct volume}}{\text{Mass flow rate in volume}}$$
$$= \frac{\text{lbm}}{\text{lbm/sec}} = \frac{\text{(kg)}}{\text{(kg/sec)}} = \text{second}$$
$$= \frac{m}{\dot{m}} \tag{9}$$

# APPENDIX

By calculating the rate of change of duct-volume total temperature in this manner, $T_{t_d}$ can be obtained from equation (7). Further, in the absence of heat addition within the duct volume itself, the total temperature at the engine face is known, since

$$T_{t_d} = T_{t_{engine\ face}} \qquad (10)$$

# REFERENCES

1.  Watson, J. M.: Engineers' Manual — Dynasar III. Rep. No. 63GL36, General Electric Co., Jan. 1, 1963.

2.  Martin, Arnold W.: Propulsion System Dynamic Simulation Theory and Equations. North American Aviation, Inc. (NASA CR 928), 1968.

3.  Martin, Arnold W.; and Wong, Heeman W.: Propulsion System Dynamic Simulation User's Manual. North American Aviation, Inc. (NASA CR 73113), 1967.

4.  Smith, Ronald H.; and Schweikhard, William G.: Initial Flight Experience With the XB-70 Air-Induction System. Proceedings of Conference on Aircraft Aerodynamics, NASA SP-124, 1966, pp. 185-194.

5.  Wolowicz, Chester H.: Analysis of an Emergency Deceleration and Descent of the XB-70-1 Airplane Due to Engine Damage Resulting From Structural Failure. NASA TM X-1195, 1966.

6.  Andrews, William H.: Summary of Preliminary Data Derived From the XB-70 Airplanes. NASA TM X-1240, 1966.

7.  Smith, Ronald H.; Bellman, Donald R.; and Hughes, Donald L.: Preliminary Flight Investigation of Dynamic Phenomena Within Air Breathing Propulsion Systems of Supersonic Aircraft. AIAA Paper No. 68-593, 1968.

8.  Martin, Richard A.: Dynamic Analysis of XB-70-1 Inlet Pressure Fluctuations During Takeoff and Prior to a Compressor Stall at Mach 2.5. NASA TN D-5826, 1970.

9.  Burcham, J.: Atmospheric Turbulence and the SST: A Review in the Light of Recent Research. Tech. Rep. 68096, British R.A.E., April 1968.

10. Ehernberger, L. J.: Meteorological Aspects of High-Altitude Turbulence Encountered by the XB-70 Airplane. Proceedings of the Third National Conference on Aerospace Meteorology, New Orleans, La., May 6-9, 1968, pp. 515-522.

11. Kordes, Eldon E.; and Love, Betty J.: Preliminary Evaluation of XB-70 Airplane Encounters With High-Altitude Turbulence. NASA TN D-4209, 1967.